RESEARCH ARTICLE OPEN ACCESS

IBFD POWER LINE COMMUNICATION FOR ANALOG INTERFERENCE CANCELLATION

J. Antony Abisha[1], & C.Rekha[2]

[1]PG scholar, ECE Department, PET Engineering College, Anna University, India
[2]Assistant Professor, ECE Department, PET Engineering College, Anna University, India

----------**********----------

Abstract:

This paper presents a basis function selection technique of a frequency-domain Hammerstein digital self interference canceller for in-band full-duplex communications. The power spectral density (PSD) of the nonlinear self-interference signal is theoretically analyzed in detail, and a nonlinear self-interference PSD estimation method is developed. The proposed selection technique decides on the basis functions necessary for cancellation and relaxes the computational cost of the frequency-domain Hammerstein canceller based on the estimated PSD of the self-interference of each basis function. Furthermore, the convergence performance of the canceller is improved by the proposed selection technique. Simulation results are then presented, showing that the proposed technique can achieve similar cancellation performance compared with the original frequency-domain Hammerstein canceller and a time-domain nonlinear canceller. Additionally, it is shown that the proposed technique improves the computational cost and the convergence performance of the original frequency-domain Hammerstein canceller.

Index Terms—Full-duplex radio, self interference, digital cancellation,Hammerstein model.

----------**********----------

I.INTRODUCTION

In this paper, we introduce a basis function selection technique for a frequency-domain Hammerstein self-interference canceller. The proposed selection technique decides basis functions necessary for cancellation and relaxes the computational cost of the frequency-domain Hammerstein canceller based on the power spectral density of the self interference of each basis function. In the proposed technique, only the nonlinear characteristics of the transmitter, which can be regarded as static, are learned in advance. To prevent degradation of cancellation performance due to variations in nonlinear characteristics, they are used for the selection of basis functions and not for training self-interference channels. Since the proposed technique can be used together with a multi-tap RF canceller, the proposed technique can be applied for much of the full-duplex hardware studied so far. Detailed equivalent baseband simulations are performed for verifying the proposed technique, and their results show that the computational cost of the frequency-domain Hammerstein canceller decreases as the power of the self interference decreases. In addition, a canceller with least square training achieves faster convergence characteristics by the proposed selection technique. Unfortunately, due to specific symbols to train the canceller, the frequency-domain Hammerstein canceller will not
be able to track channel variations simultaneously with data transmission. This problem is still not solved in this paper. However, when the symbol timing of the desired signal and the self-interference signal are synchronized, the problem does not arise because specific training symbols are unnecessary. Although this problem is very important, we treat it as a future work in this paper. The rest of this paper is organized as follows. In Section II, a detailed model of the self interference which includes nonlinearities of the IQ mixers and the power amplifier is provided. The proposed selection technique with the frequency domain Hammerstein self-interference canceller is presented in Section III. In Section IV, the performance of the proposed technique under different scenarios is analyzed with equivalent baseband signal simulations

II. SELF-INTERFERENCE SIGNAL MODEL

The Full-duplex direct-conversion transceiver model discussed in this paper. The transceiver consists of a transmitter and a receiver which have IQ mixers, RF filters, and amplifiers

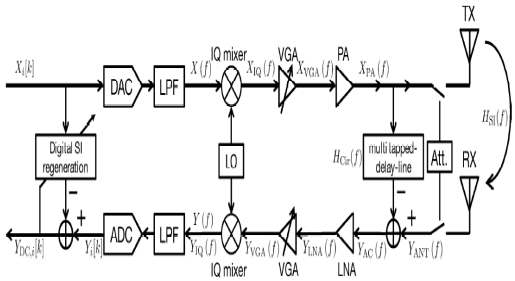

Fig: A model of full duplex tranceiver

. In addition, in the derivation of the mathematical model, we ignore the nonlinear behaviours of the LNA for simplicity, but we assume them on simulations. The nonlinear self-interference signal model has been derived on the time domain in much literature such as [13], [14], [23]. However, we describe the detailed frequency domain representation of the self interference in this section because we use it to describe our proposed scheme in the next section. The transceiver transmits an orthogonal frequency division multiplexing (OFDM) signal which has NSC subcarriers and NCP-length cyclic prefix (CP). The digital-domain discrete frequency transmit signal is expressed as Xi[k] where i and k are the symbol index and the subcarrier index, respectively. The transmit signal Xi[k] is transformed to time-domain signal x[n] by the OFDM modulator and converted to an analog baseband signal x(t) by an analog to digital converter (ADC) and a low pass filter (LPF). The analog baseband signal

$$x(t) = \sum_{\substack{k=-N_{SC}/2 \\ k \neq 0}}^{N_{SC}/2} X_i[k] e^{j2\pi k \Delta f t} \quad (t \in \mathbf{T}_i^{S} \cup \mathbf{T}_i^{CP}), \quad (1)$$

A.IQ MIXER

The analog baseband transmits signal X(f) is up converted to an RF transmit signal by the IQ mixer of the transmitter. On an ideal IQ mixer, the output equivalent baseband signal of the transmitter IQ mixer XIQ(f) is equal to the baseband transmit signal X(f). Actually, XIQ(f) has a mirror-image component of X(f) because an actual IQ mixer has imbalances between the I- and Q-phase carrier signals. The output equivalent baseband signal of the transmitter IQ mixer XIQ(f) can be

expressed as

$$X_{IQ}(f) = X(f) + b^{TX} X^{*}(f)$$

where bTX is the frequency-independent imbalance coefficient of the transmitter IQ mixer, and (.)*denotes the complex conjugate operation.

B. Power Amplifier

The output signal of the transmitter IQ mixer XIQ(f) is amplified by the VGA and transmitter because the power of XIQ(f) is very low for communication with a far away terminal. Unfortunately, nonlinear distortion of the transmit signal, which is called inter modulation distortion, will occur by nonlinearities of the PA under high transmission power. On time domain, the output signal of the PA is expressed as

$$x_{PA}(t) = h_{PA}(\tau) * \left(\sum_{p=1,3,5,\cdots}^{\infty} a_p x_{IQ}(t) |x_{IQ}(t)|^{p-1} \right)$$
$$= h_{PA}(\tau) * \left(\sum_{p=1,3,5,\cdots}^{\infty} \sum_{q=0}^{p} a_p c_{q,p-q} x^{q}(t) (x^{*}(t))^{p-q} \right)$$

((

,

C. Wireless Channel and RF Self-Interference Cancellation

The signal X PA(f) is radiated from the transmitter antenna, and is received by the receiver antenna of the same terminal as a strong self interference. The received self-interference signal YANT(f) can be expressed as

$$Y_{ANT}(f) = H_{SI}(f) X_{PA}(f) + N_{th}(f),$$

The delay-line RF self-interference canceller is composed of several passive elements such as variable attenuators, phase shifters, and delay lines. Therefore, its characteristic can be modeled as a frequency response HCir(f). The signal after the RF self-interference cancellation can be expressed as

$$Y_{AC}(f) = \{H_{SI}(f) - H_{Cir}(f)\} X_{PA}(f) + N_{th}(f),$$

III. PROPOSED SCHEME

In this section, we describe the proposed scheme based on a frequency-domain Hammerstein self-interference canceller [28]. The proposed scheme consists of three stages: pre-measurement of power ratio, training of the canceller, and cancellation. On the pre-measurement stage, we estimate the gain of the (p; q)-th nonlinear component to the linear component (GNL) as follows:

$$G_{p,q}^{N/L} = \left| \frac{a_{p+q} c_{p,q}}{a_1} \right|,$$

At the beginning of the training stage, the power of H p;q[k] p;q;i[k] is estimated based on GN/L p;q [k], and we determine whether the (p; q)-th basis function is necessary ornot. The computational cost can be reduced by the proposed basis function selection scheme because the number of the basis functions used for training is reduced.

A. Pre measurement

Since the parameters ap+q and cp;q depend on the RF circuits of the transceiver only, they can be assumed to be very static. Thus, we can measure the GNL by a massive computational resource at the time of design or when the terminal is inactive. In addition, we can use a coaxial cable and an attenuator instead of antennas and the RF cancellation circuit because the GNL does not depend on the frequency response of the self-interference channel and the RF cancellation circuits. Therefore, in this paper, we use a coaxial cable and an attenuator for loopback measurements. When the test OFDM signal xLB is used to measure the GNL, the received loopback signal can be expressed as

$$Y_i^{\mathrm{LB}}[k] = \sum_{p,q}^{\infty} H_{p,q}^{\mathrm{LB}}[k] \Psi_{p,q,i}^{\mathrm{LB}}[k] + N_i[k],$$

$$H_{p,q}^{\mathrm{LB}}[k] = a_{p+q} c_{p,q} H^{\mathrm{LB}}[k] + a_{p+q}^{*} b^{\mathrm{RX}} c_{q,p}^{*} \left(H^{\mathrm{LB}}[-k] \right)^{*}$$

B. Training

On the training stage, the swapped OFDM modulation, which is introduced in [28], is needed to estimate Hp;q[k] out of the band when the symbol timing of the desired signal and the self-interference signal are not synchronized. When the symbol synchronization is achieved, we can use pure OFDM symbols instead of swapped OFDM symbols. In the rest of this paper, we assume unsynchronized situations. The difference between synchronized and unsynchronized situations is whether the swapped OFDM modulation is used instead of pure OFDM modulation and the subcarriers used for the channel estimation. In particular, in synchronized situations, we use pure OFDM symbols and estimate the self-interference channel at k and in unsynchronized situations, we use the swapped OFDM symbols and estimate the channel at k 2 f NFFT=2;NFFT=2g where NFFT is the FFT size of the OFDM modulation. By the swapped OFDM modulation, subcarriers Xi[k] is modulated to a digital baseband signal xSWPi [n] as follows:

$$x_i[n] = \sum_{\substack{k=-N_{\mathrm{SC}}/2 \\ k \neq 0}}^{N_{\mathrm{SC}}/2} X_i[k] e^{j2\pi kn/N_{\mathrm{FFT}}} \quad (n \in [0, N_{\mathrm{FFT}}))$$

The channel response H[k] can be estimated by well-known estimation algorithms such as least squares (LS) algorithms, recursive least squares (RLS) algorithms, and normalized least mean squares (NLMS) algorithms.

1. Least squares algorithm: To apply the LS algorithm to estimate H[k], we introduce the received symbol vector and the transmit symbol matrix as respectively.

2. Recursive least squares algorithm: Since the least squares method requires matrix inversion or singular value decomposition (SVD), it may be too complicated to actually implement. On the other hand, the RLS algorithm can recursively estimate the self-interference channel which minimizes least square errors without matrix inversion and SVD

3. Normalized least mean squares algorithm: The NLMS algorithm, which has a much lower computational cost, is often used when the computational cost of the RLS algorithm produces problems such as processing speed.

4. Computational cost of the training stage: At the beginning of the training stage, the set of the basis functions J [k] is determined on each discrete frequency. In the most complicated computation is the square root, which must be computed twice at each discrete frequency.

Since it is only necessary once at the beginning of the training stage, the computational cost is sufficiently smaller than channel estimation which processes for each symbol. In the channel estimation process of the proposed scheme, received OFDM symbols are decomposed to discrete frequency components by FFT to get and it requires ½ NFFT log2 NFFT times multiplications of two complex numbers per symbol. In this paper, we assume (x[n])p(x_[n])q can be computed a priori and implemented by a lookup table. Then, the transmitted symbols are distorted by (x[n])p(x_[n])q and also decomposed to discrete-frequency components by FFT. The total computational cost of transforming symbols to the frequency domain is 1/4 (IP+2)NFFT log2 NFFT per sym symbol because FFT f(x[n])q(x_[n])pg can be computed by frequency-inversion and conjugation of FFT f(x[n])p(x_[n])qg. Next, the self-interference channel Hp;q[k] is estimated by estimation algorithms based on J [k]. The NLMS algorithm and the RLS algorithm require 2 jJ [k]j and 4 jJ [k]j2 + 4 jJ [k]j complex multiplications per discrete frequency per symbol, respectively

IV. NUMERICAL SIMULATIONS

In this section, we provide numerical simulation results to verify the proposed scheme. To show the effectiveness of the proposed scheme, we compare the performance of the proposed scheme with a conventional

A. Simulation environment

To verify the proposed scheme, equivalent baseband simulations of the full-duplex transceiver performed. The baseband signal simulator is implemented with the D programming language, where each non-ideality is modeled with realistic behaviours Since the dynamic range of the receiver ADC is about 79 dB under these simulation parameters [33], the largest barrier to self-interference cancellation is nonlinear distortions of IQ mixers and the PA. The PA nonlinearities are realized by the Rapp model [34], [35], which is often used to simulate class AB solid state power amplifiers

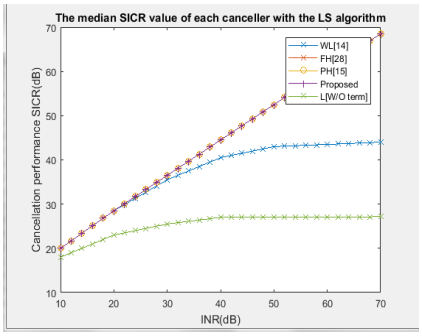

Fig : 4.1 The median SICR value of each cancellation with LS algorithm

The median cancellation performance of all trials on each canceller with the LS algorithm is shown at N Tr = 60 and SLNA = 3. The time-domain linear canceller, which is implemented based without the conjugated term x, cannot reconstruct the nonlinear self-interference signal. Hence the cancellation performance of the linear canceller is saturated at about 22 dB. Hence, by the proposed basis function selection technique, the self-interference cancellation performance of the frequency-domain Hammerstein

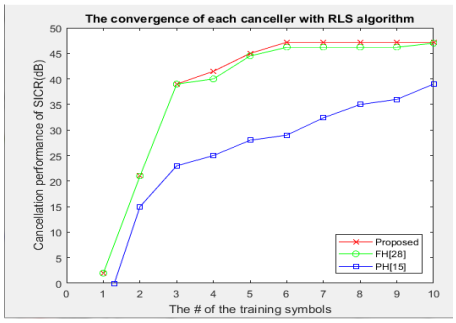

Fig: 4.2 The median SICR value of each canceller with the R LS algorithm

The convergence performance of each canceller with the LS algorithm is shown at INR = 50 dB. The proposed technique improves the initial convergence speed of the frequency-domain Hammerstein canceller, and it achieves better cancellation performance than the conventional method when the number of training symbols NTr is less than eight. By removing the basis functions unnecessary for self-interference cancellation by the proposed technique, the number of parameters of the canceller decreases, and convergence performance is improved.

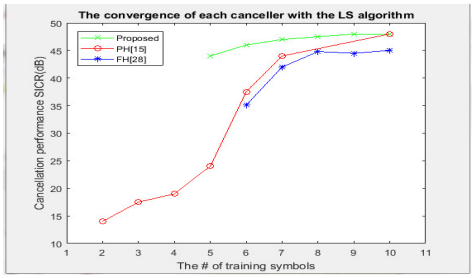

Fig : 4.3 The convergence of each canceller with LS algorithm

The convergence performance of each canceller with RLS algorithm is shown at INR = 50 dB. In contrast with the case of the LS algorithm, the frequency-domain cancellers predominantly show better convergence performance than the time-domain nonlinear canceller. In the time domain, the input signal of the canceller is strongly colored, and convergence speed of an adaptive algorithm decreases with a colored input signal. However, the input

signal of an adaptive algorithm of the frequency-domain Hammerstein canceller is almost white, and the convergence speed of them is faster than that seen in the time-domain case.

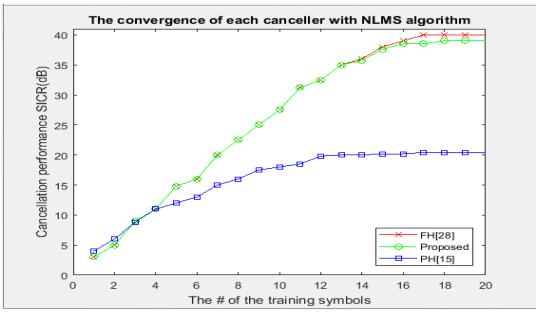

Fig :4.4 The convergence of each canceller with NLMS algorithm

V. CONCLUSION

In the proposed method a basis function selection technique of the frequency-domain Hammerstein self-interference canceller for in-band full-duplex communication systems. The estimation technique of the power spectral density of the received self-interference is developed from the detailed nonlinear characteristics of a full-duplex terminal. The proposed selection technique reduces unnecessary basis functions for cancellation before the training stage according to the estimated self-interference power at each discrete frequency. Simulation results show that the proposed technique improves computational cost and convergence performance of the original frequency-domain Hammerstein canceller. It is shown that computational cost can be reduced to about one fifth in the low self-interference situation by reducing the basic functions according to the estimated self-interference signal power. In addition, by the proposed basis function selection technique, self-interference cancellation performance of the frequency-domain Hammerstein canceller hardly decreases and achieves similar cancellation performance compared with the original.

REFERENCES

[1] G. Prasad, L. Lampe, and S. Shekhar, "Enhancing transmission efficiency of broadband PLC systems with in-band full duplexing," in IEEE Intl. Symp. Power Line Commun. And it's Appl. (ISPLC), March 2016.

[2] A. Sabharwal, P. Schniter, D. Guo, D. W. Bliss, S. Rangarajan, and R. Wichman, "In-band full-duplex wireless: Challenges and opportunities," IEEE J. Sel. Areas Commun., vol. 32, no. 9, pp. 1637–1652, 2014.

[3] S. Weinstein, "Echo cancellation in the telephone network," IEEE Commun. Mag., vol. 15, no. 1, pp. 8–15, January 1977.

[4] A. G. Stove, "Linear FMCW radar techniques," in IEE Proceedings FRadar and Signal Processing, vol. 139, no. 5. IET, 1992, pp. 343–350.

[5] M. Ho, J. M. Cioffi, and J. A. Bingham, "Discrete multitone echo cancelation," IEEE Trans. Commun., vol. 44, no. 7, pp. 817–825, 1996.

[6] R. Mahadevan, "A front-end circuit for full-duplex transmission over coaxial cable." Ph.D. dissertation, University of Toronto, 2001.

[7] T.-C. Lee and B. Razavi, "A 125-MHz mixed-signal echo canceller for gigabit ethernet on copper wire," IEEE J. Solid-State Circuits, vol. 36, no. 3, pp. 366–373, 2001.

[8] "IEC 62488-1:2012: Power line communication systems for power utility applications," International Electro technical Commission.[Online]. Available:https://webstore.iec.ch/publication/7095

[9] G. Prasad, L. Lampe, and S. Shekhar, "In-band full duplex broadband power line communications," IEEE Trans. Commun., vol. 64, no. 9, pp. 3915–3931, Sept 2016.

[10] J. I. Choi, M. Jain, K. Srinivasan, P. Levis, and S. Katti, "Achieving single channel, full duplex wireless communication," in ACM MOBICOM, 2010, pp. 1 1

[11] M. Duarte, C. Dick, and A. Sabharwal, "Experiment-driven characterization of full-duplex wireless systems," IEEE Trans. Wireless Commun., vol. 11, no. 12, pp. 4296–4307, 2012.

[12] E. Tsakalaki, E. Foroozanfard, E. De Carvalho, and G. F. Pedersen, "A 2-order MIMO full-duplex antenna system," in IEEE European Conf. Antennas and Propagation (EuCAP), 2014.

[13] A. Sahai, G. Patel, and A. Sabharwal, "Pushing the limits of full-duplex: Design and real-time implementation," arXiv preprint arXiv: 1107.0607, 2011.

[14] E. Everett, A. Sahai, and A. Sabharwal, "Passive self-interference suppression for full-duplex infrastructure nodes," IEEE Trans. Wireless Commun., vol. 13, no. 2, pp. 680–694, 2014.

[15] C. J. Kikkert, "Coupling," in Power Line Communications: Principles, Standards and Applications from Multimedia to Smart Grid, L. Lampe, A. Tonello, and T. Swart, Eds. John Wiley and Sons Ltd, 2016, ch. 4, pp. 223 – 260.

[16] D. Bharadia, E. McMillan, and S. Katti, "Full duplex Radios," in ACM SIGCOMM, 2013, pp. 375–386.

[17] Y.-S. Choi and H. Shirani-Mehr, "Simultaneous transmission and reception: Algorithm, design and system level performance," IEEE Trans. Wireless Commun, vol. 12, no. 12, pp. 5992–6010, 2013.

[18] M. Duarte and A. Sabharwal, "Full-duplex wireless communications using off-the-shelf radios: Feasibility and first results," in 44th Asilomar Conference on Signals, Systems and Computers (ASILOMAR). IEEE, 2010, pp. 1558–1562.

.

